On the factors affecting the high temperature insulator-metal transition in rare-earth manganites

2001 J. Phys.: Condens. Matter 13 L431

(http://iopscience.iop.org/0953-8984/13/20/106)

INSTITUTE OF PHYSICS PUBLISHING JOURNAL OF PHYSICS: CONDENSED MATTER

J. Phys.: Condens. Matter **13** (2001) L431–L439 www.iop.org/Journals/cm PII: S0953-8984(01)20876-5

LETTER TO THE EDITOR

On the factors affecting the high temperature insulator–metal transition in rare-earth manganites

Dipten Bhattacharya[1,3], Pintu Das[1], A Pandey[1], A K Raychaudhuri[1,4], Amitava Chakraborty[2] and V N Ojha[1]

[1] National Physical Laboratory, New Delhi 110 012, India
[2] Electroceramics Division, Central Glass & Ceramic Research Institute, Calcutta 700 032, India

E-mail: dipten_bhattacharya_2000@yahoo.com

Received 12 January 2001, in final form 2 April 2001

Abstract

The measurement of resistivity (ρ) across a wide temperature (T) range—from 15 to 1473 K—in the rare-earth manganite series of compounds reveals a very interesting feature: the normally observed insulating pattern beyond T_c (the Curie point) undergoes a broader transition and eventually gives way to a reentrant metallic pattern around a characteristic temperature T^*. Considering a model with coexisting metallic and non-metallic phases beyond T_c, it has been shown that T^* marks the temperature at which the metallic volume fraction $v_m(T)$ reaches 100% as a result of progressive removal of lattice distortion at higher temperature. T^* is found to be dependent on the carrier concentration as well as on the average A-site radius ($\langle r_A \rangle$) for a fixed carrier concentration.

In recent years the physics of rare-earth manganites (with general chemical formula $Re_{1-x}Ae_xMnO_3$; Re = La, Nd, Pr etc and Ae = Sr, Ca, Ba etc) has attracted considerable interest as this series of compounds displays a number of fascinating phenomena, such as colossal magnetoresistance (CMR), charge ordering (CO), magnetic field driven insulator–metal transition, electronic phase segregation etc, across the entire phase diagram. A fine interplay of charge, spin and orbital effects is responsible for most of the observed phenomena. A very crucial issue in the physics of manganites is the onset of lattice distortions at high temperature; one such distortion is the cooperative Jahn–Teller (JT) effect around the Mn^{3+} ions in $Mn^{3+}O_6$ octahedra. The onset of lattice distortion at high temperature (typically at $T > 500$ K) is believed to be the cause of the insulating state that occurs in these oxides in the paramagnetic state. It has been observed that the parent compound $LaMnO_3$ undergoes a cooperative transition associated with removal of JT distortion around the Mn^{3+} ions at $T \approx 750$ K (referred to as T_{JT}) as seen through neutron diffraction [1]. A recent transport measurement in single crystals of $LaMnO_3$ shows that at the same temperature the resistivity

[3] Corresponding author. Currently at Electroceramics Division, Central Glass & Ceramic Research Institute, Calcutta 700 032, India.
[4] Currently at the Department of Physics, Indian Institute of Science, Bangalore 560 012, India.

0953-8984/01/200431+09$30.00

(ρ) drops by nearly two orders of magnitude on heating through T_{JT} and it becomes temperature independent beyond T_{JT} [2]. The magnetization data indicate a discontinuous rise in Weiss constant which signifies a concomitant rise in ferromagnetic interactions in Curie–Weiss paramagnetism beyond T_{JT}. It is thus clear that, at least, in the parent compound $LaMnO_3$, for $T > T_{JT}$, as the orbital order due to the JT effect is removed, one does get a phase with sharply reduced resistivity. This certainly marks the onset of a qualitatively new phase at T_{JT}. In the absence of a better description we call this a high temperature 'reentrant metallic phase'.

Past experimental works on bivalent metal ion substituted systems like $Re_{1-x}Ae_xMnO_3$ (where Re changes from La to Ho and Ae = Ca, Sr, Ba, Pb) have, in fact, shown evidence of even an upturn in the ρ versus T curve at characteristic high temperatures (T^*) which has been described as an indication of a reentrant metallic phase [3, 4]. We refrain, at this stage, from identifying T^* as T_{JT} since T^* is found to be dependent on other factors as well, apart from the JT effect. An understanding of the occurrence of the reentrant metallic phase at high temperature is of fundamental importance because this can elucidate the role of lattice distortion in the CMR oxides, particularly at higher temperatures ($T > T_c$). At $T > T_c$, due to the presence of strong coupling of the lattice distortion to carrier hopping, the transport is governed by a small polaronic hopping mechanism and ρ shows an activated behaviour with $\rho = \rho_0 T^\alpha \exp(E_a/k_B T)$ [5]. Of course, it appears that the conduction mechanism in this temperature regime may switch from that of a pure small polaronic hopping to one of a mixture of metallic and polaronic transport (because of a phase segregation) depending on the extent of lattice distortion—larger distortion may give rise to pure small polaronic transport while smaller distortion may lead to a mixture of metallic and polaronic conduction. In the latter case, the transition can take place locally over a large temperature range above T_c and the onset of reentrant metallic resistivity behaviour around T^* implies completion of a transition process. The transition at T^* is thus the completion of a change in the transport mechanism—from a mixed metallic and small polaronic mechanism to metallic conduction. In this letter, we report the results of our preliminary investigation regarding the nature of a transition process from an insulating phase to a metallic phase across the entire temperature range: T_c to T^*. We have shown that the metallic volume fraction v_m within the insulating matrix increases steadily with temperature in a regime beyond T_c and reaches 100% at around T^*. We also identify the parameters that might govern the temperature T^* in a series of rare-earth manganites. It is important to note that the metallic phase envisaged here is distinct from band metal and has rather high resistivity. This type of metallic phase with high resistivity has been seen before in a number of oxide materials where the conductivity $\sigma \leqslant \sigma_{Mott}$, σ_{Mott} being the Mott minimum metallic conductivity [6]. The conduction in this phase can be due to large polaron transport.

The experiments were carried out on well sintered, single-phase bulk pellets. A range of compositions, such as $La_{1-x}Ca_xMnO_3$ (x = 0.2–0.5), $Re_{0.5}Ae_{0.5}MnO_3$ (Re = Nd, Y and Ae = Ca and Sr) etc, were prepared for this investigation. In addition, we utilized the results of our earlier investigation [4]. The powder (of approximate size 0.5 μm) was prepared by autoignition of citrate–nitrate gel. This method allows preparation of powder at a rather low temperature [7]. The powders thus obtained were calcined at 1273–1373 K for 24 h and finally sintered at around 1650 K for 10 h in pellet form. The phase purity, microstructure as well as compositional homogeneity of all the samples were studied by x-ray diffraction, scanning electron microscopy and energy dispersive x-ray spectra. Thermogravimetric analysis carried out until 1473 K could not detect any weight loss; 1473 K is the highest temperature attained during the resistivity measurements. The resistivities of the samples were measured in the temperature range 15–1473 K using the usual four-probe technique. At high temperatures we used platinum paste (Make Tanaka KK, Japan) to make the contacts with the thin platinum leads. The contacts were cured at greater than 1000 °C overnight. The magnetization of the

samples over 15–300 K was measured in a vibrating sample magnetometer (DMS 1660).

All the samples depicted expected resistivity and magnetization patterns within the temperature range 15–300 K. For example, the $La_{1-x}Ca_xMnO_3$ ($x = 0.2$–0.5) series exhibits the usual ferromagnetic and metallic transitions (T_c) at temperatures in the range 200–270 K. These values of T_c closely agree with those found previously in these compounds [8].

Typical resistivity data over 15–1473 K are shown in figure 1 for a few important compositions of $La_{1-x}Ca_xMnO_3$ ($x = 0.2$, 0.3, 0.4, 0.45, 0.5). It can be seen that at a certain temperature T^* (beyond T_c), the resistivity patterns shown an upturn and it increases as T is increased beyond T^*. The temperature T^* is identified from the point where the derivative $d\rho/dT \geqslant 0$. The onset of reentrant metallic behaviour and the pattern beyond are shown clearly in the inset of figure 1. One rather interesting point may be noted from figure 1 in that in almost all the samples studied the reentrant metallic transition takes place around a resistivity value of 5–9 mΩ cm. In fact, for a large class of ABO_3 type perovskite oxides, the insulator–metal transition takes place for $\rho \approx 1$–10 mΩ cm [6]. For many of these oxides, as stated earlier, a metallic phase exists with even higher resistivity and such a phase often shows a $\rho \propto T$ pattern.

As is evident from figure 1, the upturn in the resistivity pattern around T^* is not preceded by a sharp drop in resistivity as was observed in pure $LaMnO_3$. The general behaviour is a very flat pattern before the upturn. It appears, therefore, that although T^* marks a transition, the transition process may have been set at an even lower temperature. In other words, the transition might be quite broad. In order to see the nature of the transition and charge conduction mechanism over the entire temperature range T_c to T^*, we consider a model with coexisting metallic and insulating phases above T_c. We propose that the total current is divided between the coexisting phases, giving rise to an effective conductivity which is dependent on the relative strength of the two. The effective conductivity $\sigma_{eff}(T)$ in such a model is given by

$$\sigma_{eff}(T) = v_m\sigma_m(T) + (1 - v_m)\sigma_{ins}(T) \tag{1}$$

where σ_m is the conductivity of the metallic phase ($\sigma_m = (a + bT)^{-1}$; a, b are constants), v_m is the metallic volume fraction and σ_{ins} is the conductivity of the insulating phase ($\sigma_{ins} = (\sigma_0/T)\exp(-E_a/k_BT)$; E_a is the transport activation barrier for small polaronic hopping conduction). We have assumed that σ_m follows the relation $(a + bT)^{-1}$. This relation has been taken to phenomenologically describe the decreasing conductivity of the anomalous metallic phase with T. Such a pattern has been observed in many oxides and other strongly correlated systems, most notably in the high-T_c superconducting oxides over a wide temperature range ~100–1000 K [9]. By fitting the metallic and insulating parts of the resistivity pattern (figure 1) with the respective equations we determine the parameters a, b, σ_0 and E_a/k_B. The value of the temperature coefficient of resistivity 'b/a' determined from the fit (given in the caption of figure 2) is around 10^{-3} to 10^{-4} K^{-1} which is very often seen in high-resistive metallic systems. The difference between the values of the parameter 'b' observed in the two representative compounds—$La_{0.7}Ca_{0.3}MnO_3$ and $La_{0.5}Ca_{0.5}MnO_3$—can be attributed to the difference in the extent of disorder prevalent in the metallic phase. The charge disorder can be higher in the former compound (than in the latter) because of the random distribution of the dopants in this low doping range [10]. Finally, we determine the temperature dependence of v_m by considering all other parameters as being temperature independent. In figure 2 we show the pattern of variation of $v_m(T)$ with temperature. It is quite interesting to note that $v_m(T)$ rises steadily with temperature in the regime beyond T_c and reaches 100% at around T^*. It clearly shows that a transition from insulating to metallic phase is set at a much lower temperature than T^*. T^* only marks the completion of the transition process. *The removal of lattice distortion, therefore, takes place progressively over the entire temperature range right*

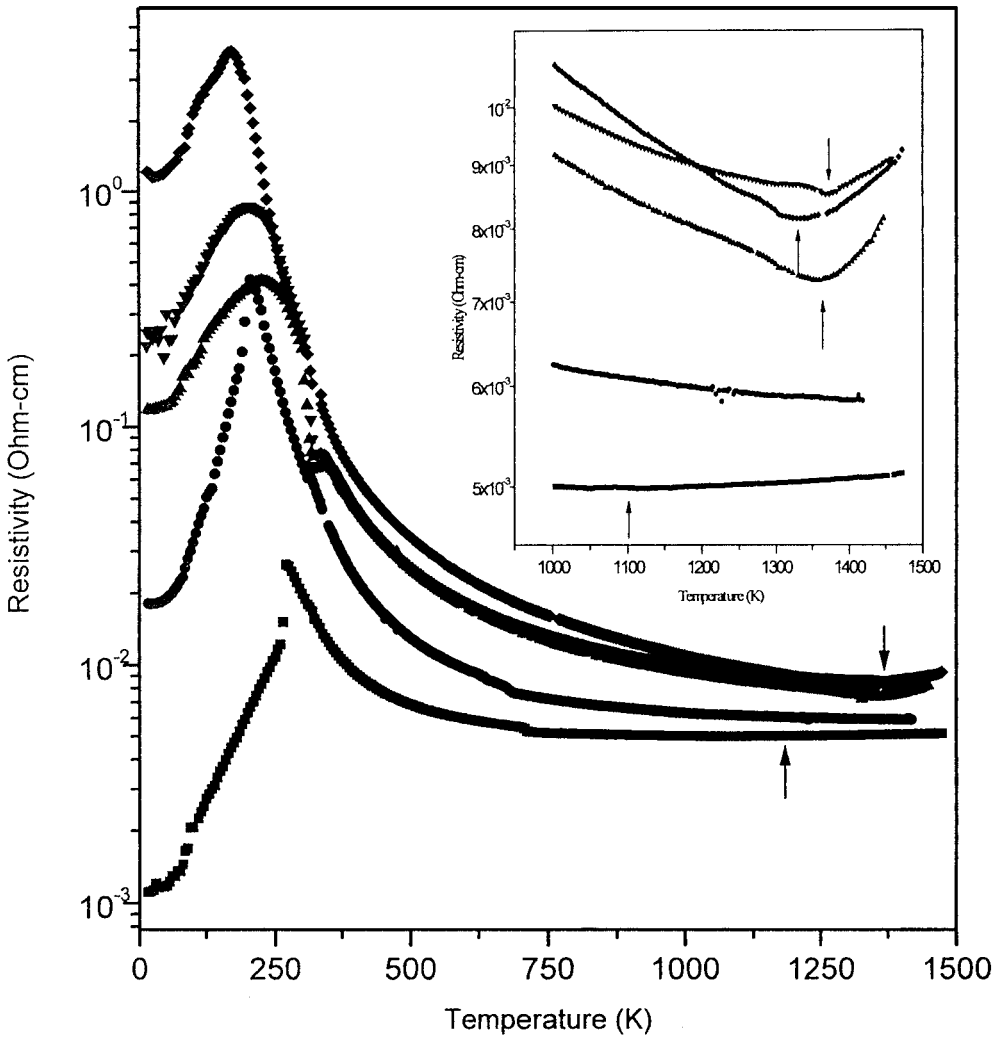

Figure 1. The resistivity versus temperature plots over a regime 15–1473 K for some of the important compounds: $La_{0.8}Ca_{0.2}MnO_3$ (●), $La_{0.7}Ca_{0.3}MnO_3$ (■), $La_{0.6}Ca_{0.4}MnO_3$ (▲), $La_{0.55}Ca_{0.45}MnO_3$ (▼) and $La_{0.5}Ca_{0.5}MnO_3$ (♦). Inset: the onset of the insulator–metal transition around T^* and the resistivity pattern beyond T^*.

up to T^*. This scenario can be easily contrasted with the nature of the transition observed in the case of pure $LaMnO_3$, where a sharp drop in resistivity and change in resistivity pattern takes place at a particular temperature T_{JT} [2]. The reason behind such a broader transition in our case could be a distribution in the lattice distortion and dopants across the entire matrix. In fact, incorporation of dopants can also lead to a disorder [10]. It is important to point out that the presence of a finite metallic volume fraction $v_m(T)$ below T^* is an indication that the conduction mechanism here does not strictly follow the small polaronic hopping scenario. In an earlier work [5], the signature of the pure small polaronic mechanism is observed in Hall coefficient versus temperature data in a series $(La_{1-x}Gd_x)_{0.67}Ca_{0.33}MnO_3$ whose average A-site radius $\langle r_A \rangle$ is ∼1.13 Å. In the series explored in our work, the $\langle r_A \rangle$ values vary between

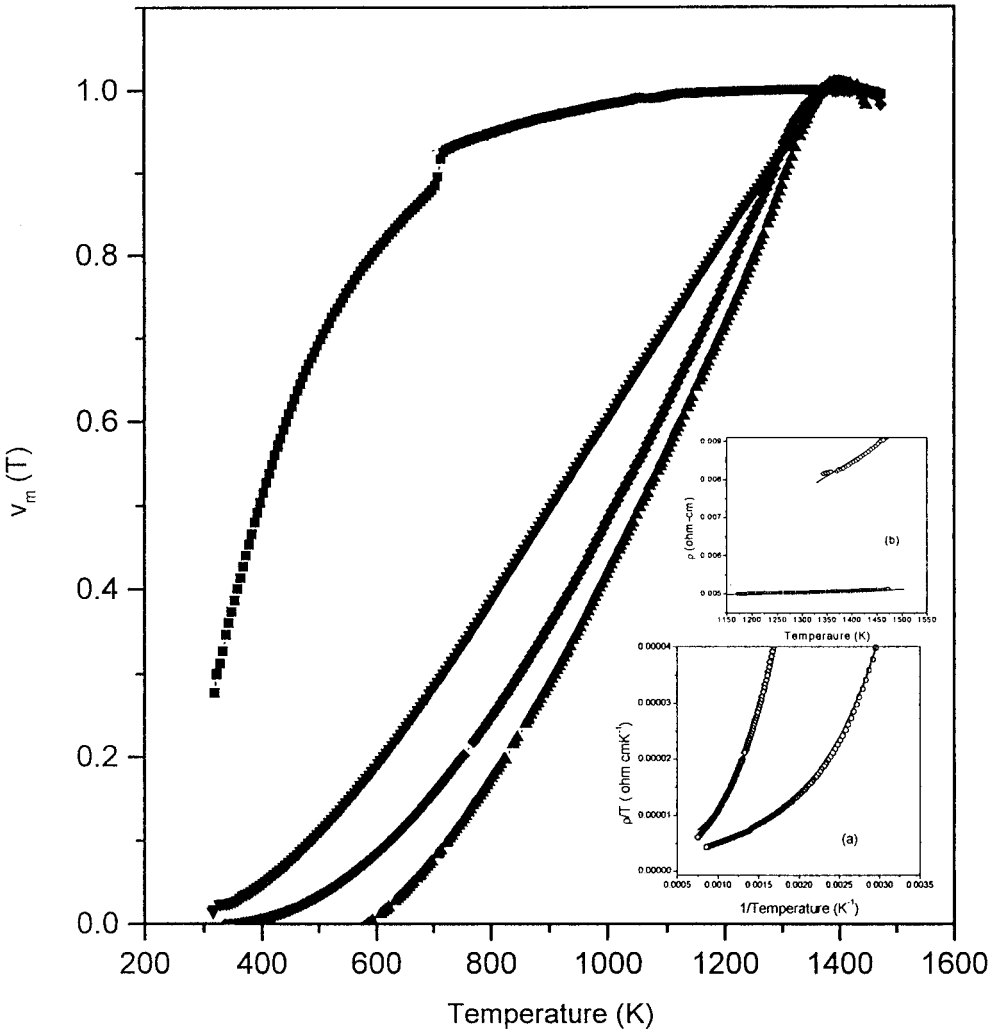

Figure 2. The variation of metallic phase volume fraction $v_m(T)$ with temperature for the compounds: $La_{0.7}Ca_{0.3}MnO_3$ (■); $La_{0.6}Ca_{0.4}MnO_3$ (▲); $La_{0.55}Ca_{0.45}MnO_3$ (▼); $La_{0.5}Ca_{0.5}MnO_3$ (▼). Insets: (a) the insulating part of the resistivity pattern for $La_{0.7}Ca_{0.3}MnO_3$ (○) and $La_{0.5}Ca_{0.5}MnO_3$ (◇) with the fitting curves (——); the fitting parameters are $\rho_0 = 4.08 \times 10^{-6}$, 7.21×10^{-6} Ω cm and $E_a/k_B = 1099$, 1748 K, respectively; (b) the metallic part of the resistivity patterns for the same samples; the fitting parameters are $a = 0.0045$, 0.0029 Ω cm and $b = 3.8 \times 10^{-7}$, 8.16×10^{-6} Ω cm K^{-1}, respectively, for both samples.

1.17 and 1.26 Å. Therefore, it seems that beyond a threshold $\langle r_A \rangle$ one has coexisting insulating and metallic phases between T_c and T^*, and the conduction mechanism undergoes a change from pure small polaronic hopping conduction to a mixed metallic and polaronic conduction as one crosses the threshold $\langle r_A \rangle$.

The charge conduction in the metallic state above T^* (after completion of the process of lattice distortion removal) may follow the large polaron transport mechanism where the charge carriers are coupled with larger multi-site distortion. Since the large polaron transport takes place coherently with lesser scattering, the ρ–T pattern exhibits a metallic behaviour [11].

The pattern may be linear in T as observed in the case of high-T_c superconductors [9]. The transition in the ρ–T pattern over T_c to T^* can, therefore, be considered as a small polaron to large polaron transition. The value of the conductivity σ is $\approx\sigma_{Mott}$, as observed in a large class of perovskite oxides where strong on-site correlation governs the insulator–metal transition [6].

We have also observed the dependence of T^* on parameters like carrier concentration and bandwidth of the manganite system. In figure 3, we show the variation of T^* as a function of carrier concentration (x) for the series $La_{1-x}Ca_xMnO_3$ (LCMO) and $La_{1-x}Sr_xMnO_3$ (LSMO). We incorporate the T_{JT} data of the parent compound $LaMnO_3$. For the sake of completeness, we have also included results of earlier studies carried out on LCMO for $x > 0.5$ (marked in the figure caption). It can be immediately seen that the dependence of T^* on x is not monotonous and it shows a peak at $x = 0.45$ for LMCO and $x = 0.25$ for LSMO. This is an anomalous pattern. It points out that the transition temperature T^* does not depend on the JT effect alone. It also highlights the fact that even though one observes a sharp drop in resistivity at T_{JT} in the parent $LaMnO_3$, in other compounds T_{JT} and T^* may signify two different transitions and, therefore, they may or may not coincide in a given compound. It can be mentioned, in this context, that detailed lattice distortion and phase transition studies at high temperature [1] in the parent $LaMnO_3$ compound point out the presence of lattice distortion even beyond T_{JT} ($\sim$750 K) and a second phase transition at around 1010 K. It will be interesting to investigate the onset of upturn in the resistivity pattern, if any, in this compound as *the upturn in the resistivity pattern at high temperature can only be observed when all types of lattice distortions are removed*. Therefore, we emphasize that T^* depends on other types of lattice distortions as well apart from the JT effect. One such distortion is the mismatch in the A-site size which leads to the tilting and rotation of the MnO_6 octahedra and consequent modulation in the conduction bandwidth. The possibility of the presence of other types of distortion and their influence on T^* provides an explanation of the difference in behaviour between the LCMO and LSMO series. The bending of the Mn–O–Mn bonds due to tilting and rotation of MnO_6 octahedra is greater in the former case than in the latter ($\langle r_A\rangle$ is less in the former case). Hence, the anomalous T^* versus x pattern is extended up to a higher x value in the former series. It will be interesting to study the difference and/or coincidence of T_{JT} and T^* for all the compositions by studying, separately, the removal of JT and other distortions through structural studies and the onset of resistivity upturn through resistivity measurements. However, for higher values of x, T^* does decrease with increasing x as expected. *This result clearly shows that the carrier concentration (or the concentration of JT-active Mn^{3+} ions) alone does not determine T^* although it must be one of the determining factors*.

In the region $0.2 < x \leqslant 0.5$, both LCMO and LSMO samples show a ferromagnetic transition and the onset of metallic behaviour at T_c. In the presence of a double exchange interaction (DEI), the metallic state is stabilized by the ferromagnetic interaction below T_c. T_c, of course, depends on x as well as $\langle r_A\rangle$. The bandwidth of the conduction band, in such a regime, is proportional to T_c and T_c is generally taken as a measure of bandwidth. The same samples show reentrant metallic behaviour for $T \geqslant T^*$. The insulating state is thus stable in the temperature range $T^* - T_c$ ($= W$). As the bandwidth increases, T_c increases and the increased metallicity weakens the local JT distortion and thus destabilizes the insulating state. The enhanced bandwidth is thus expected to reduce the temperature range W over which the insulating state is stable. In order to see a direct correlation, if any, between W and the DEI-governed bandwidth, we plot W versus $1000/T_c$ in figure 4. It can be seen that W drops initially with $1000/T_c$ which implies that a smaller bandwidth compound has low T_c and high T^*. For sufficiently small bandwidth, the ferromagnetic state is not stable and gives way to charge and

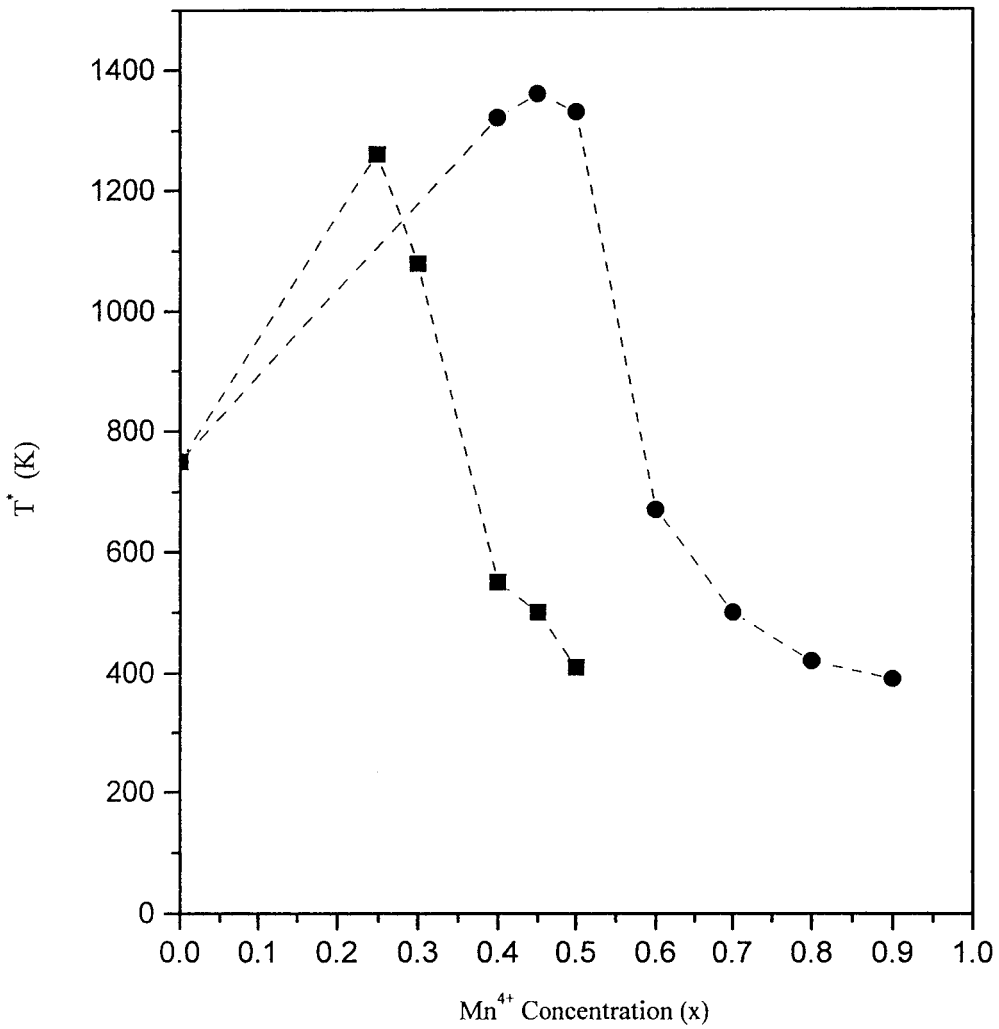

Figure 3. Variation of T^* with carrier concentration (x) for the $La_{1-x}Sr_xMnO_3$ (■) and $La_{1-x}Ca_xMnO_3$ (●) series. The data for the LCMO series in the range $x > 0.5$ are taken from [3].

orbital order along with an antiferromagnetic order. A logical conclusion would be that for a sufficiently large bandwidth, $W \rightarrow 0$, i.e. $T^* \rightarrow T_c$. However, the W versus $1000/T_c$ data show that W is minimum for an optimum T_c and not maximum T_c. For even higher T_c, W rises again. The presence of such a minimum points out that large bandwidth (i.e. large T_c) alone (where the bandwidth is primarily governed by DEI) does not guarantee stability of the metallic state. The minimum in the plot is observed for a composition $La_{0.5}Sr_{0.5}MnO_3$, whereas for the composition $La_{0.7}Sr_{0.3}MnO_3$ (whose T_c is even higher) W is higher. The stability of the insulating state (as measured by W), therefore, is related to the concentration of JT-active Mn^{3+} ions as well. Even in a compound of very high T_c, W can be quite high if the concentration of JT ions is large. On the other hand, it can be observed that W drops monotonically with x in the LSMO series which shows that W has a one-to-one correspondence with x in such a large bandwidth system (see inset (a) of figure 4).

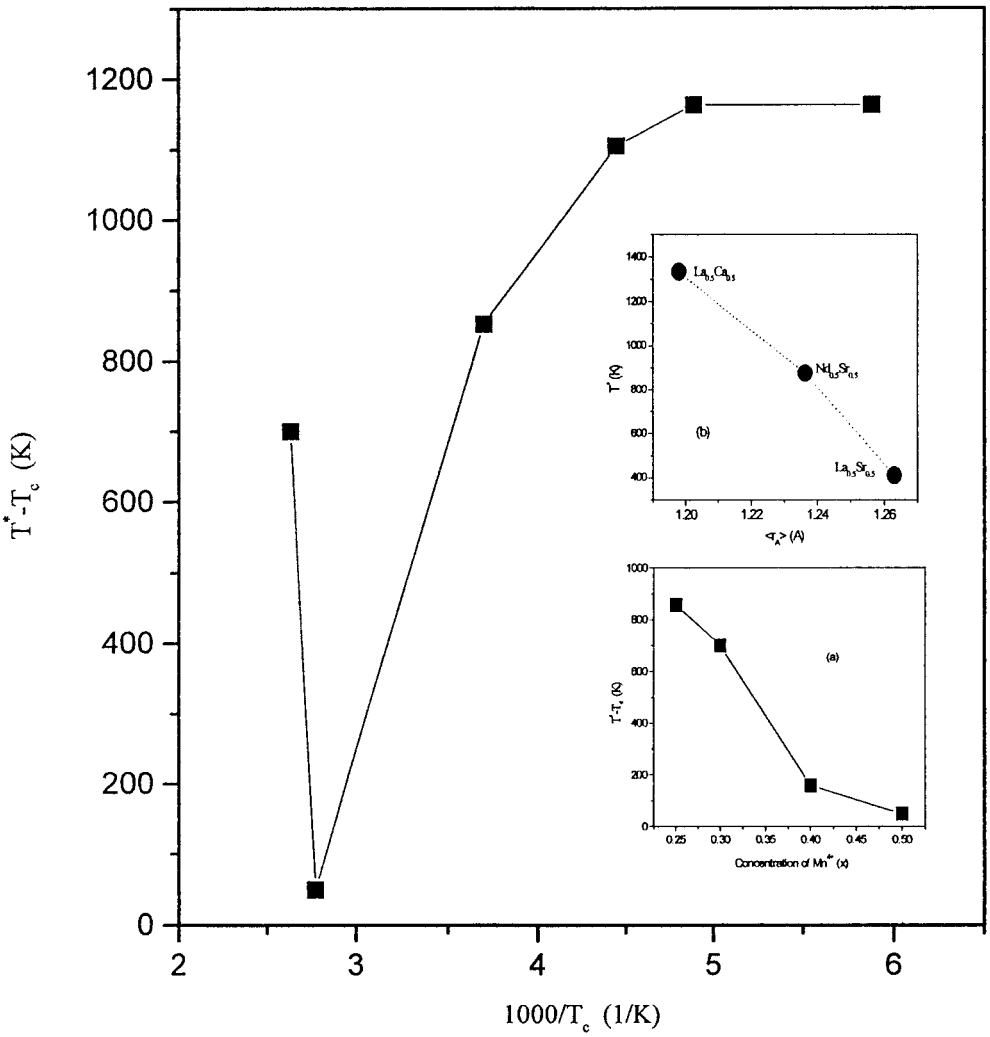

Figure 4. Variation of W $(= T^* - T_c)$ with $1000/T_c$ in the compounds depicting both the ferromagnetic metallic to paramagnetic insulating transition as well as the high temperature insulator–metal transition. Insets: (a) variation of W with the concentration of Mn^{4+} ions and (b) variation of T^* with $\langle r_A \rangle$.

The dependence of T^* on another important parameter, $\langle r_A \rangle$, can be seen, separately, if we fix x and vary $\langle r_A \rangle$, a factor that is known to control the packing of the MnO_6 octahedron (geometric effect) and can be linked to the bandwidth. A larger $\langle r_A \rangle$ ensures a larger bandwidth. In the inset (b) of figure 4, we show T^* as a function of $\langle r_A \rangle$ for a fixed value of x, namely, $x = 0.5$. We have defined $\langle r_A \rangle = (r_{Re} + r_{Ae})/2$ for the composition $Re_{0.5}Ae_{0.5}MnO_3$; r_{Re}, r_{Ae} data are taken from a table of Shannon [12]. It can be very clearly seen that T^* drops with the rise in $\langle r_A \rangle$ for a given carrier concentration.

These results point out that two factors that appear to control T^* (or the high temperature insulator–metal transition), more significantly, are the carrier concentration (or the concentration of the JT-active Mn^{3+} ions) and the A-site size mismatch (geometric factor)

or bandwidth for a fixed x. It will be interesting to observe an interplay, if any, between these two kinds of lattice distortions—(i) JT and (ii) geometric. From a detailed local structural distortion study, one can unravel the extent of interplay, if any. This, however, is beyond the scope of this present work.

In summary, we have provided data on the insulator–metal transition (and removal of lattice distortion) at higher temperature (beyond T_c) in a series of rare-earth manganites. We have shown that, specific to the compositions studied in this work, the transition is quite broad, extending over almost the entire temperature range T_c to T^*. T^* only marks the temperature at which the transition from insulating to metallic phase is complete. We have also pointed out that T^* depends on the carrier concentration (x) or the concentration of JT-active Mn^{3+} ions, the DEI-governed bandwidth as well as on the geometric factor (A-site size mismatch) for compounds with fixed x and T^* varies from $T^* \gg T_c$ to $T^* \rightarrow T_c$. However, in the absence of a detailed structural study, it may not always be possible to separate out the influence of any particular factor. Our study underscores the need to carry out such high temperature measurements in order to estimate the effective lattice distortion which governs the CMR and CO effects etc significantly. It will be interesting to study any interplay between the JT effect and the geometric effect through estimation of the nature and extent of local lattice distortion. This issue will be addressed in a future work.

The authors acknowledge thankfully the assistance rendered by A K Halder and S K Pratihar (CGCRI) during the high temperature resistivity measurements. They also acknowledge the support of R G Sharma (NPL) and H S Maiti (CGCRI). One of the authors (AKR) acknowledges the financial support from BRNS and two other authors (PD and AP) acknowledge financial support from UGC and CSIR, Government of India.

References

[1] Rodriguez-Carvajal J, Hennion M, Moussa F, Moudden A H, Pinsard L and Revcolevschi A 1998 *Phys. Rev.* B **57** R3189
[2] Zhou J S and Goodenough J B 1999 *Phys. Rev.* B **60** R15 002
[3] Kobayashi T, Takizawa H, Endo T, Sato T, Shimada M, Taguchi H and Nagao M 1992 *J. Solid State Chem.* **92** 116
[4] Bhattacharya D, Chakraborty A and Maiti H S 1999 *J. Phys.: Condens. Matter* **11** 5845
[5] Jaime M, Hardner H T, Salamon M B, Rubinstein M, Dorsey P and Emin D 1997 *Phys. Rev. Lett.* **78** 951
[6] Raychaudhuri A K 1995 *Adv. Phys.* **44** 21
[7] Chakraborty A, Devi P S and Maiti H S 1995 *J. Mater. Res.* **10** 918
[8] See, for example, Schiffer P, Ramirez A P, Bao W and Cheong S-W 1995 *Phys. Rev. Lett.* **75** 3336
[9] See, for example, Dagotto E 1994 *Rev. Mod. Phys.* **66** 763
[10] Martin I and Balatsky A V 2000 *Preprint* cond-mat/0011252
[11] Emin D 1995 *Polarons and Bipolarons in High-T_c Superconductors and Other Related Materials* ed E K H Salje, A S Alexandrov and W Y Liang (Cambridge: Cambridge University Press) p 80
[12] Shannon R D 1976 *Acta Crystallogr.* A **32** 751